Published online 1 March 2010

Nucleic Acids Research, 2010, Vol. 38, No. 12 ***4079–4091***
doi:10.1093/nar/gkq109

Identification of a structural element of the hepatitis C virus minus strand RNA involved in the initiation of RNA synthesis

Kathleen Mahias[1], Neveen Ahmed-El-Sayed[1], Cyril Masante[1], Juliette Bitard[1], Cathy Staedel[2], Fabien Darfeuille[2], Michel Ventura[1] and Thérèse Astier-Gin[1,*]

[1]CNRS UMR 5234 and [2]INSERM U869, IFR66, Université Bordeaux 2, 146 rue Léo Saignat, 33076 Bordeaux cedex, France

Received June 23, 2009; Revised February 5, 2010; Accepted February 7, 2010

ABSTRACT

The replication of the genomic RNA of the hepatitis C virus (HCV) of positive polarity involves the synthesis of a replication intermediate of negative polarity by the viral RNA-dependent RNA polymerase (NS5B). *In vitro* and likely *in vivo*, the NS5B initiates RNA synthesis without primers. This *de novo* mechanism needs specific interactions between the polymerase and viral RNA elements. *Cis*-acting elements involved in the initiation of (–) RNA synthesis have been identified in the 3′ non-coding region and in the NS5B coding region of the HCV RNA. However, the detailed contribution of sequences and/or structures of (–) RNA involved in the initiation of (+) RNA synthesis has been less studied. In this report, we identified an RNA element localized between nucleotides 177 and 222 from the 3′-end of the (–) RNA that is necessary for efficient initiation of RNA synthesis by the recombinant NS5B. By site-directed mutagenesis experiments, we demonstrate that the structure rather than the primary sequence of this domain is important for RNA synthesis. We also demonstrate that the intact structure of this RNA element is also needed for efficient RNA synthesis when the viral NS5B functions in association with other viral and cellular proteins in cultured hepatic cells.

INTRODUCTION

Hepatitis virus C (HCV) is a virus of the *Flaviviridae* family that induces severe liver diseases in human (1). The viral genome is a single-stranded RNA of positive polarity containing a single open reading frame (ORF) flanked by the two untranslated regions (UTRs), the 5′UTR and 3′UTR (2). Translation of the ORF is initiated through an internal ribosome entry site (IRES) present in the 5′UTR (3). The polyprotein produced after complete ORF translation is cleaved by cellular and viral proteases to generate the structural proteins (capsid, C and envelopes, E1 and E2) and seven non-structural proteins (p7, NS2, NS3, NS4A, NS4B, NS5A and NS5B). In hepatoma cells, the nonstructural proteins assemble with cellular proteins (4) in a cell compartment derived from the endoplasmic reticulum, termed 'membranous web' (5), to form the replication complex (RC) responsible for viral RNA synthesis (6). The catalytic subunit of the RC is the NS5B protein that harbors an RNA-dependent RNA polymerase activity *in vitro* (7,8) but it has been shown that the NS3 to NS5B proteins are necessary for viral RNA synthesis in hepatoma cells (9). The 3′UTR is composed of a short variable region, a polypyrimidine tract (poly U-UC) of variable length and a highly conserved 98-nt segment (3′X). The two latter domains are essential for viral infectivity *in vivo* (10) and RNA replication of HCV replicons (11,12).

During HCV RNA replication, the viral RC synthesizes a minus-strand RNA that serves as a template for the synthesis of new plus-strand RNA molecules. *In vitro* and most probably *in vivo*, the NS5B polymerase initiates RNA synthesis by a *de novo* mechanism at the 3′-end of the plus and minus strand RNA (13–16). Initiation of RNA synthesis involves interactions between the protein components of the replication complex, in particular with the viral polymerase (NS5B), and structures and/or sequences of the viral RNA templates. The involvement of the three stem–loops of the 3′X has been extensively studied both in cell culture using the replicon system and *in vitro* (11,12,17). More recently, it has been reported that

*To whom correspondence should be addressed. Tel: +33 5 57 57 17 42; Fax: +33 5 57 57 17 66; Email: therese.astier@u-bordeaux2.fr

cis-acting elements present at the 3′-end of the NS5B coding region form long-range RNA–RNA interactions necessary for HCV replication (18–20). The secondary structure of the 3′-end of the minus-strand RNA complementary of the 5′UTR has been also established (21,22) but the detailed contribution of sequences and/or structures in the RNA synthesis has been less studied. The 222 nt at the 3′-end fold in 5 stable stem–loops that are identical in the two models. Conversely, the structure of upstream sequences is less stably organized and depends on the length of the analyzed RNA (23). We have previously shown that the 341 nt of the 3′-end of the minus strand RNA are efficiently replicated by purified HCV NS5B *in vitro* and that initiation occurs by a *de novo* mechanism on the 3′ cytosine (24). This high level of RNA synthesis relies on sequences and/or structures present near the 3′-end but also on upstream domains (25). Comparable observations were made in a cellular system using a HCV replicon for which it was shown that the 125 nt at the 3′-end of the minus strand RNA were sufficient for RNA synthesis, but that the 341 nt were needed to obtain an optimal level of replication of the replicon (26,27).

In the present work, we investigated in detail the role of the sequence and structure of the SL-E1 stem–loop formed by nucleotides 177–222 from the 3′-end of the HCV minus strand RNA, first *in vitro* by using model RNAs and a recombinant NS5B protein and then in Huh7 cells harboring the viral RC.

MATERIALS AND METHODS

RNA templates

The 341-nt-long RNA corresponding to the 3′-end of the minus-strand RNA was synthesized by *in vitro* transcription of DNA template obtained by polymerase chain reaction (PCR) amplification from the pGEM-T 439 containing the 439 nt of the 5′-end of pCV-H77 (28) kindly provided by J. Bukh (NIH, Bethesda, Maryland, USA). The PCR primers 5′S7 and 5′341T7-2 were designed to introduce a T7 RNA polymerase promoter in the correct orientation (Table S1). PCR was performed with the Ampli*Taq* gold DNA polymerase kit (Perkin Elmer). *In vitro* transcripts were synthesized using the MEGAscript kit (Ambion). DNA templates were digested with DNase I for 15 min. After phenol/chloroform extraction, the RNAs were precipitated with isopropanol and 0.5 M ammonium acetate. The purity and the integrity of synthesized RNAs were determined by analysis on a 6% polyacrylamide gel containing 7 M urea in TBE buffer (90 mM Tris–borate pH 8.0, 1 mM EDTA). All RNA mutants were obtained by modification of the 5′ UTR sequence contained in the pGEM-T 439 using the QuikChange Site-Directed Mutagenesis Kit (Stratagen) and oligonucleotides described in Table S2. The sequence of mutated fragments was verified by DNA sequencing using the ABI Prism Big Dye terminator sequencing kit.

RdRp assay

The recombinant HCV NS5B-Δ21 of HCV J4 (genotype 1b) expressed in *Escherichia coli* and purified as previously described (25) was used in all experiments. The assay was performed in a total volume of 20 µl containing 20 mM Tris–HCl pH 7.5, 1 mM DTT, 5 mM $MgCl_2$, 40 mM NaCl, 17 U RNasin (Promega), the 3 rNTP (ATP, CTP and GTP) 0.5 mM each, 86 nM of RNA template, 200 nM of purified NS5B and either 10 µCi [α-^{32}P]UTP (3000 Ci × mmol^{-1}, Amersham Pharmacia Biotech) and 2 µM UTP or 2 µCi [^{3}H]UTP (46 Ci × mmol^{-1}). The reaction mixture was incubated for 2 h at 25°C and stopped by addition of 10% trichloracetic acid (TCA). The radioactivity incorporated into neo- synthesized RNA was then determined by scintillation counting. To quantify and analyze the ^{32}P-labeled RNA, the synthesis was stopped by adding 6.25 mM EDTA, 10 mM Tris–HCl pH 7.5 and 0.125% SDS. An aliquot of the reaction products was precipitated by 10% TCA and the radioactivity incorporated in neo-synthesized RNA was determined as above. The remainder of the products was purified by phenol/chloroform extraction (1/1 vol/vol) and precipitated by 1 vol of isopropanol in the presence of 0.5 M ammonium acetate. RNAs were dissolved in 95% formamide, 0.5 mM EDTA, 0.025% SDS, 0.025% bromophenol blue, 0.025% xylene cyanol and then heated for 2 min at 94°C. The same amount (50 000 c.p.m.) of each sample was loaded onto a 6% polyacrylamide denaturing gel containing 7 M urea in TBE buffer. After electrophoresis, the labeled RNA products were visualized by electronic autoradiography with a Pharos apparatus (Biorad).

For single-round replication assay, HCV RdRp and RNA were pre-incubated for 30 min at 25°C in the same reaction mixture as above but without ATP and UTP. Heparin (MW 4000–6000 Da, 200 µg/ml), then ATP and [^{32}P]UTP were successively added. The reaction mixture was further incubated at 25°C for 0, 5, 10, 20 or 60 min. The ^{32}P RNA products were quantified after TCA precipitation or analyzed on polyacrylamide gels as described in the above paragraph.

Gel-based initiation assay

The assay was carried out in 20 µl of 20 mM Tris pH 7.4, 50 mM NaCl, 5 mM $MgCl_2$, 1 mM DTT, 0.4 U/µl RNasin, 1 µM RNA template, 1 µM NS5B. The initiation phase was analyzed by adding 0.5 mM GTP and 10 µM CTP with 4 µCi [α-^{32}P] CTP (3000 Ci mmol^{-1}) only. At different time points, 4 µl were collected, the reaction was quenched by adding 1 µl of 100 mM SDS and diluted in 8 µl of formamide/dyes loading buffer. After denaturation at 70°C for 5 min, samples were loaded onto a 20% polyacrylamide gel in TBE buffer containing 7 M urea. The migration was performed at 30 W for 3 h and the gel was submitted to electronic autoradiography. The pppGpC molecular weight marker was synthesized as previously described (29).

Gel shift assay

RNAs were labeled by *in vitro* transcription using the MEGAscript kit (Ambion) and 15 μCi [α-^{32}P]UTP (Amersham Pharmacia Biotech). The amount of radioactivity incorporated into the nucleic acids was measured by precipitating 2-μl aliquots with 10% TCA and counting in a Wallac scintillation counter. RNAs were precipitated with isopropanol and dissolved in water.

Labeled RNA was thermally denatured for 2 min at 94°C, and then quickly cooled on ice for 5 min. RNA at a concentration of 13 nM (10 000 c.p.m.) was renatured at 25°C for 10 min in 9 μl RdRp reaction mixture (without NTP) before adding 200–1600 nM of enzyme (in a 1-μl volume). The incubation was continued for 20 min at 25°C. Two microliters of electrophoresis loading buffer (10 mM Tris pH 8.0, 1 mM EDTA, 0.1% bromophenol blue, 0.1% xylene cyanol, 30% glycerol) were added to the samples before loading onto a non-denaturing 4% polyacrylamide gel (acrylamide:bis acrylamide 59/1). The samples were run at 200 V at room temperature. The gel was autoradiographied and scanned using the NIH Image J program. The percentage of bound RNA was plotted against the concentration of NS5B. The apparent K_d (kd_{app}) is defined as the concentration of the NS5B resulting in 50 % shifting of [^{32}P] RNA.

^{32}P RNA labeling at the 5′- and 3′-ends

For 5′-end ^{32}P labeling, *in vitro* transcribed RNAs were dephosphorylated with calf intestine alkaline phosphatase (Roche) following the manufacturer's instructions. The dephosphorylated RNA was labeled with [γ-^{32}P] ATP and T4 polynucleotide kinase (Promega) according to standard procedure and purified with GeBAflex-tube dialysis and extraction kit (Gene Bio-Application) after electrophoresis on 6% polyacrylamide denaturing gel.

For 3′-end ^{32}P labeling, RNAs with a deletion of the 3′C were synthesized *in vitro* as described above and labeled with [^{32}P]pCp (Amersham Pharmacia Biotech) and T4 RNA ligase following the standard procedure. The labeled RNAs were purified as described above.

Primer extension and sequence with labeled primers

Control or modified RNAs (0.2 μg) was mixed with ^{32}P labeled probe (5×10^5 c.p.m.) in a 9 μl final volume, denatured for 1 min at 90°C, quickly cooled on ice and incubated for 5 min at room temperature. Reverse transcription was performed by using SuperScript II following the manufacturer instructions (Invitrogen) at 45°C for 30 min in a final volume of 15 μl. The reaction was stopped by adding 20 μl of stop solution (50 mM Tris–HCl pH 8.5, 0.1% SDS). The RNA was hydrolyzed by treatment with 0.4 M KOH for 3 min at 90°C and 3 h at 37°C. After neutralization, DNA was precipitated by ethanol and 0.3 M sodium acetate. The sequence reaction was performed by using the Thermo Sequenase Cycle sequencing Kit (USB Corporation). Labeled products were analyzed on an 8% polyacrylamide denaturing gel containing 7 M urea in TBE buffer.

Nuclease mapping

^{32}P-labeled RNAs (100 000 c.p.m.) in 4 μl H_2O were denatured by heating at 94°C for 1 min and cooled on ice for 1 min and then at room temperature for 5 min. RNA were then renatured for 10 min at room temperature after addition of 2 μl of 5X buffer (final concentration: 20 mM Tris–acetate pH 7.6, 5 mM magnesium acetate and 100 mM sodium acetate) and 1 μl tRNA (1 μg/μl). The reaction volume was adjusted to 10 μl after addition of 1 μl of RNase T1 (0.25 U/μl, Ambion) and samples incubated at 37°C for 5 min. After precipitation by adding 10 μl 0.3 M ammonium acetate and 90 μl ethanol, the reaction products were collected by centrifugation and dissolved in 7 μl of gel loading buffer II (Ambion). For each RNA sample, a control reaction was performed in the same reaction buffer without RNase T1. RNase T1 digestion in denaturing condition and alkaline hydrolysis of ^{32}P-labeled RNAs (100 000 c.p.m.) were performed with buffers and conditions described with RNase T1 (Ambion). The different reaction products were heated at 94°C for 2 min and loaded on an 8% polyacrylamide 8 M urea denaturing gel, 3 μl were run for 1.5 h and 3 μl were run for 2.5 h at 75 W. After migration, the gels were dried and autoradiographied with a hyperfilm MP (Amersham Pharmacia Biotech).

Chemical probing

Before reaction with Pb^{2+} ions, DEPC or DMS, RNAs were denatured at 94°C for 1 min and then renatured for 10 min at room temperature after addition of 5× buffer.

Lead cleavage. ^{32}P-labeled RNA (100 000 c.p.m.) and yeast RNA (1 μg) in 20 mM HEPES-NaOH pH 7.5, 5 mM magnesium acetate, 50 mM potassium acetate and 25 mM lead acetate were incubated for 1 min at 20°C in a 10 μl final volume. The reaction was stopped by adding 30 μl of gel loading buffer (95% formamide, 7 mM EDTA, 0.025% SDS and 0.025% bromophenol blue and xylene cyanol). A control reaction in the same reaction buffer without lead addition was performed with each RNA preparation.

DEPC modification. The reaction in native conditions was performed in a 20 μl reaction mixture containing ^{32}P-labeled RNA (100 000 c.p.m.) and yeast RNA (2 μg) in 25 mM Tris–HCl pH 7.5, 5 mM $MgCl_2$ and 25 mM KCl. One microliter of DEPC was then added. After incubation for 20 min at room temperature, RNA was precipitated by sodium acetate and ethanol. DEPC modification in denaturing conditions was performed in 25 mM HEPES-NaOH pH 7.5, EDTA 1 mM and DEPC (same concentration as above) for 1 min at 70°C to 90°C as indicated in the figure legend. After ethanol precipitation, RNAs were dissolved in 10 μl 1 M aniline pH 4.6 and incubated for 10 min at 60°C. After precipitation with ethanol, the RNAs were dissolved in gel loading buffer and analyzed on polyacrylamide gel as above. When DEPC modifications were monitored by primer extension, 1 μg of unlabeled RNA and 1 μg of yeast RNA were incubated in a 20-μl reaction mixture containing 25 mM

Tris–HCl pH 7.5, 5 mM $MgCl_2$ and 25 mM KCl. One microliter of DEPC was then added. After incubation for 20 min at room temperature, RNAs was precipitated by sodium acetate and ethanol and used in primer extension experiments. A control reaction in the same reaction buffer without DEPC addition was performed with each RNA preparation.

DMS modification. RNA (1 μg) and yeast RNA (1 μg) were incubated for 10 min at room temperature in a 20 μl solution containing 25 mM Tris–HCl pH 7.5, 5 mM $MgCl_2$ and 25 mM KCl and 1 μl of DMS (1/8 dilution in ethanol). The reaction products were precipitated by ethanol as above and used in primer extension experiments. A control reaction in the same reaction buffer without DMS addition was performed with each RNA preparation.

Cell culture and transfection

All cell lines were cultured in Dulbecco's modified Eagle medium supplemented with 10% heat-inactivated fetal calf serum and gentamycin (50 μg/ml) at 37°C in a 5% CO_2 H_2O saturated atmosphere. The Huh7-QR and Huh7/Rep5.1 cell lines, HCV RC-negative and HCV RC-positive respectively, have been previously described (30,31). For transfection experiments, 24 h before transfection, 10^5 of the appropriate cells were seeded in 24-well plates. RNA transfection was performed by using DMRIE-C (Invitrogen) according to the manufacturer's protocol.

Translation and luciferase assay

The pIRF plasmid (32) was used to evaluate the IRES activity of wild type (WT) and mutated HCV 5′UTR. The original pIRF plasmid was modified by inserting the HCV 3′UTR downstream from the Renilla gene as described by Dumas *et al*. (33). The first 368 bp of the HCV H77 DNA were PCR-amplified with primers Bam_5UTR and Pst1-439 (Supplementary Table S1) that introduced a BamH1 and a Pst1 site at the 5′- and at the 3′-ends, respectively. After digestion with the restriction enzymes, the DNA fragments were introduced upstream of the Renilla luciferase into the pIRF plasmid cleaved by the same enzymes. After DNA sequencing to verify the sequence, the pIRF plasmids were linearized with Xho1 and used as templates for *in vitro* RNA transcription with the Amplicap T7 Kit (Epicentre Biotechnology). The RNA were transfected into Huh7-QR cells as described above and the enzymatic activities of the Firefly (Fluc) and the Renilla (Rluc) luciferases were measured by using the Dual-Luciferase Reporter assay system (Promega) 24 h after transfection.

Minigenome replication assay

The minigenome construct pGEM-T/5UTR-H2AE-3UTR has been previously described (30). The basic construct contains the 5′UTR, the first 27 nt of the core coding sequence and the 3′UTR of HCV Con1. These three domains were first replaced by those of the HCV H77. Sequences of the H77-HCV 3′UTR were PCR-amplified with primers Xba_3UTR_H77 and Sph1_3UTR_stop (Table S1) and Taq fusion polymerase (Finnzyme) to introduce Xba1 and Sph1 restriction sites at the 5′- and 3′-ends, respectively. After cleavage by the restriction enzymes, the fragment was inserted at the same sites in the pGEM-T/5UTR-H2AE-3UTR to give the pGEM-T/5UTR-H2AE-$3UTR_{H77}$. Sequences of the H77-HCV 5′UTR were amplified from the pGEM-T 439 with the SpeI_5UTR_H77_st and Corefus_BamH1_Stop (Supplementary Table S1) to insert the Spe1 and BamH1 site at the 5′- and 3′-ends, respectively. After cleavage by the restriction enzymes, the fragment was introduced between the same restriction sites of the pGEM-T/5UTR-H2AE-$3UTR_{H77}$ to give the pGEM-T/$5UTR_{H77}$-H2AE-$3UTR_{H77}$. Mutated 5′UTR were introduced in the same way instead of the WT 5′UTR. The RNA transcripts from wild type and mutated $5UTR_{H77}$-H2AE-$3UTR_{H77}$ were obtained as previously described (30), except that an acidic phenol treatment was added after incubation with DNase I to eliminate all DNA templates. The RNA minigenomes were transfected into Huh7/Rep5.1 cells (four wells of 24-well plates for each construct) as described above. Sixteen hours after transfection, the percentage of transfected cells from two wells was evaluated by flow cytometry as previously described (30). Forty-eight hours after transfection, the two remaining wells were trypsinized, transferred to Petri dishes (100 mm diameter) and maintained for 3 weeks in DMEM medium supplemented with 500 μg/ml G418 and 50 μg/ml hygromycin. Colonies were stained with Coomassie brilliant blue (2.5 g/liter in 45% methanol and 10% acetic acid).

Northern blot analysis

Total cellular RNAs were isolated using the TRIzol Reagent (Invitrogen) following the manufacturer's instructions. RNA (10 μg) obtained from Huh7/Rep5.1 cells 4 h after transfection were denatured in MOPS buffer (20 mM MOPS pH 7, 5 mM sodium acetate, 0.5 mM EDTA), 50% formamide, 2.2 M formaldehyde for 15 min at 55°C. After electrophoresis in a 1% agarose gel in MOPS buffer 2.0 M formaldehyde, RNAs were transferred by capillarity in 20 SSC (3 M NaCl, 0.3 M sodium citrate) onto nylon membrane (Hybond N, Amersham Pharmacia Biotech) and UV cross-linked. Membranes were hybridized with ^{32}P-labeled EGFP or GAPDH probes as previously described (33). The ^{32}P-EGFP probe was synthesized with Prime-It II Random Primer labeling Kit (Stratagene) using a 520-bp DNA template obtained by PCR with EGFP-S3 and EGFP-AS3 primers (Supplementary Table S1). The ^{32}P-GAPDH probe was synthesized following the same procedure from a 232-bp DNA template obtained by PCR with GAPDH (+) and GAPDH (–) primers (Supplementary Table S1). After hybridization, the nylon membrane was washed as previously described (33) and labeled bands visualized using a Pharos apparatus (Biorad).

RESULTS

Mutations in the SL-E1 domain decreased *in vitro* RNA synthesis

Earlier studies showed that sequences and/or structures in the 125 nt at the 3′-end of the HCV minus strand RNA are important for RNA synthesis *in vitro* (24,25,34) and in Huh7 cells (26,27). However, data from the same groups and of Van Leeuwen and colleagues (35) indicated that upstream sequences were necessary to obtain a high level of RNA synthesis. To identify these sequences more precisely, we decided to investigate the role of the SL-E1 stem–loop formed by nucleotides 177–222 from the 3′-end of this RNA for two reasons. First, we have previously shown that hybridization of antisense oligonucleotides to the region comprised between nucleotides 216 and 255 from the 3′-end strongly inhibits *in vitro* RNA synthesis (36). Second, the 3′ border of the apical loop of the hairpin formed by nucleotides 177 and 222 (named SL-E1 or IIIb′) bears a 6-nt sequence (GAAAGG) homologous to the SL II stem–loop of the 3′X present in the plus strand RNA (21,22). Synthesis was performed by using an RNA template corresponding to the 341 nt of the 3′-end from the HCV minus strand RNA and a recombinant NS5B deprived of the 21 C-terminal amino acids. Nucleotide changes were introduced in the apical loop and in the upper part of the stem to modify the sequence homologous to the loop of SLII of the 3′UTR, and at the bottom of the stem to destabilize the sequence where inhibitory antisense oligonucleotides hybridized (Figure 1A). The mutants were designed so that the base changes did not alter the secondary structures of the other domains of the 341 nt RNA as determined with the RNADraw software.

As shown with the mutants G192A-G193A (2GA), A194U-A195U-A196U (3AU) and G197C (GC), changes of 1–3 residues in the upper part of the stem–loop did not decrease RNA synthesis (Figure 1B). A slight increase in RNA synthesis was even observed with 2GA and 3AU mutants. Even when all six residues homologous to SLII (SLE1AL mutant) were changed, RNA synthesis was unaffected as compared to wild-type (WT) RNA. Conversely, mutations G218A-G219A (2A mutant) and G218A-G219A plus G177A-G178A (4A mutant) that were predicted to disrupt the lower part of the helix reduced RNA synthesis by 53% and 48%, respectively. Altogether, these data suggested that the structure rather than the sequence of SL-E1 stem–loop contributed to efficient replication of this template RNA.

To test this hypothesis, we constructed another RNA mutant for which the 2 C residues at positions 180 and 181 were changed to U so as to restore base-pairing in the 2A mutant (2AU mutant). As shown in Figure 1B, these modifications completely restored the level of RNA synthesis, strongly suggesting that the native structure of this RNA domain is important for efficient RNA synthesis from the 3′end of the HCV minus strand RNA by the NS5B polymerase *in vitro*.

RNA structure probing of wild-type and mutant RNAs

To confirm that nucleotide modifications introduced into 2A and 4A mutants induced a structural change of SL-E1 stem, we compared their folding with that of the wild-type 341 nt RNA. To do this, RNAs were subjected to lead cleavage, DEPC modification and partial digestion with T1 RNase as illustrated in Supplementary Figures S1–S5. The model of secondary structure of the 341 nt of the WT RNA derived from these experiments and from secondary

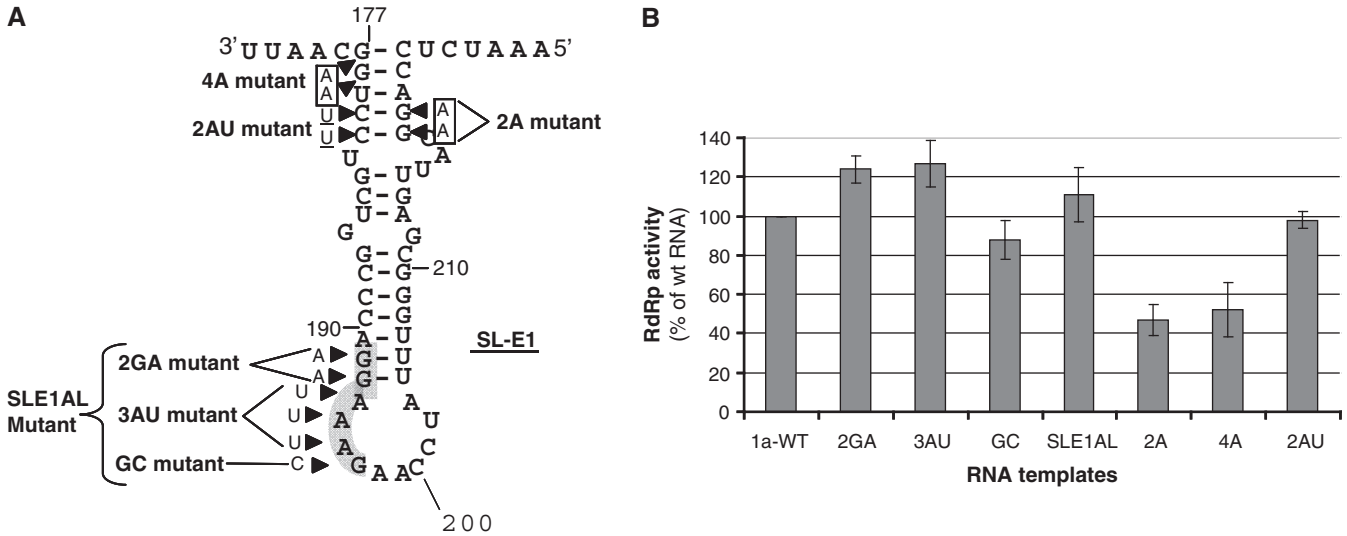

Figure 1. Some mutations in the SL-E1 stem–loop decreased *in vitro* RNA synthesis by NS5B. (**A**) Secondary structure of SL-E1 stem–loop. Arrow heads indicate the position of the nucleotide changes. Sequence homologous to SLII stem–loop is filled in grey. (**B**) An RdRp assay was performed with the purified NS5B1b (200 nM) and mutant RNAs as templates as described in 'Materials and Methods' section. The amount of RNA synthesized was determined after TCA precipitation and counting in a Wallac scintillation counter. The results were expressed as the percentage of the value obtained with the WT RNA (mean ± SD, $n = 3$ independent experiments).

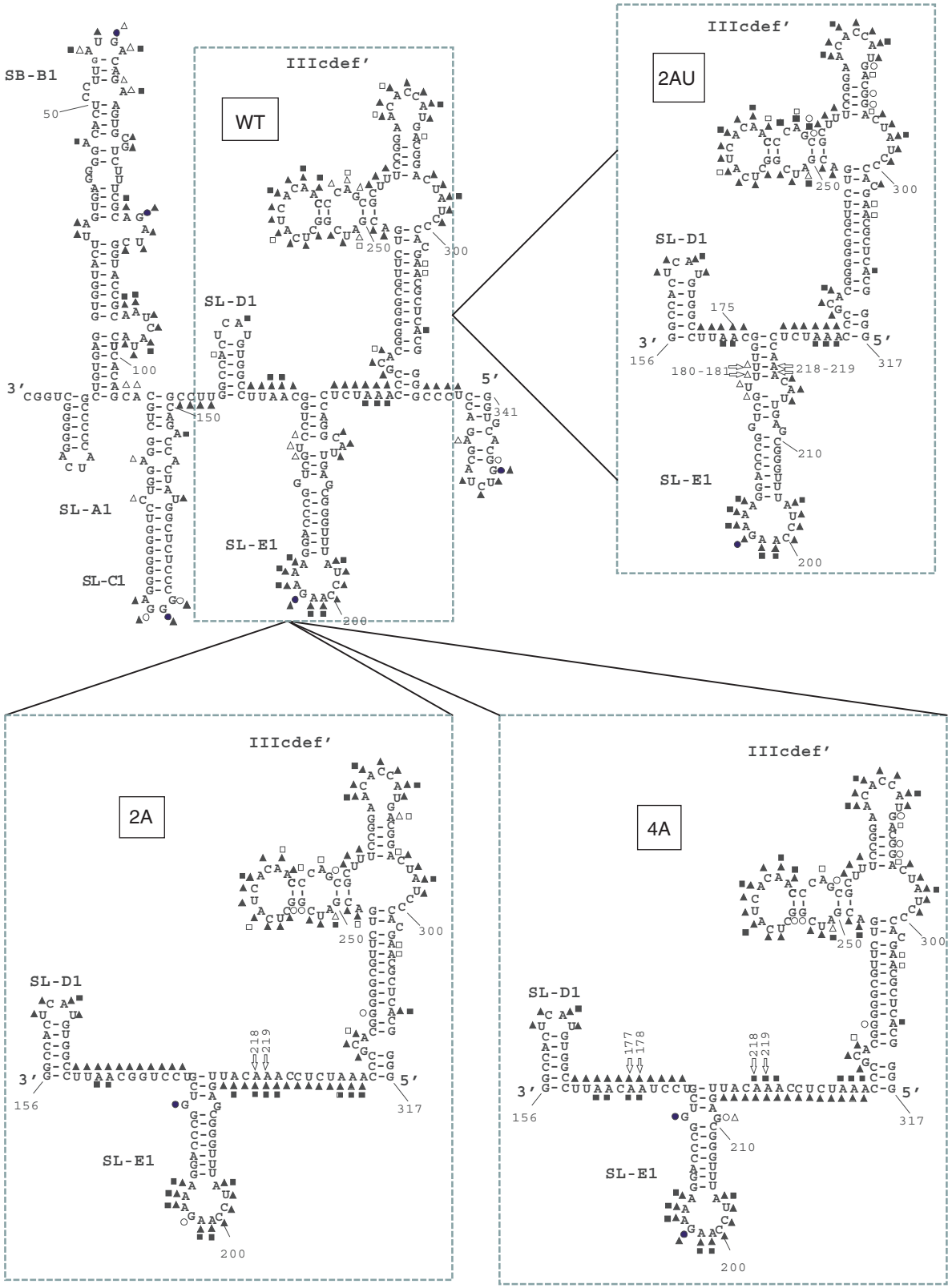

Figure 2. Secondary structure models of WT and 2A, 4A and 2AU mutant 341 nt RNAs. WT RNA: The first 222 nt (numbered from 3′-end) of the 341 nt WT fold in five stem–loops identical to those proposed by Schuster *et al.* (21) and Smith *et al.* (22). The same notation as in (21) was used. The 223–317-nt sequence fold in a structure similar to the IIIcdef' structure presented by Smith *et al.* (22). Lead reactivity is represented by triangles, RNase T1 reactivity is represented by circles and DEPC reactivity is represented by squares. Empty or filled symbols are for weak or strong cleavage, respectively. 2A, 4A and 2AU RNAs: a close-up section of the model secondary structures of nt 156 to nt 317 are shown. Reactivity is indicated by the same symbols. The positions of A and U residues introduced by mutations of G or C residues are indicated by arrows.

structure predictions *in silico* is presented in Figure 2 (WT). This RNA fragment folded in seven stem–loops. The 3′ 222 nt were arranged in five stem–loops as in the three previous published models (21–23). Upstream sequences (nt 223–341) contained two short single-stranded regions and two stem–loops. The first one (nt 229–317 from the 3′-end) contained four bulges and a 7-nt apical loop. This model is very similar to the structure arrangement of the IIIcdef' stem–loop proposed by Smith *et al.* (22), with the exception of the apical part. Indeed, The G280 and G289 and the A281 and the A290 were not reactive or only poorly to RNase T1, lead or DEPC, suggesting that they could form G-A pairs or interact with other RNA domains (in red in Supplementary Figure S1 and S2B and D and Supplementary Figure S4C and D). The same analysis was done with 2A, 4A and 2AU mutant RNAs. A close-up section of the structure spanning nucleotides 156–317 is boxed in rectangles in Figure 2. They showed that residues 177–181 and 218–222 were sensitive to lead cleavage or DEPC modification in 2A and 4A RNAs compared to WT or 2AU compensatory mutant RNA. The residues of other domains of the mutants RNA displayed a similar reactivity to enzymatic or chemical probing indicating that they were not modified by mutations introduced in the SL-E1 domain (Supplementary Figure S1–S4 and Figure 2). To further confirm that the G to A mutation of residues 218 and 219 in 2A mutant induced also a mismatch of the A220-U179 adjacent base pair, DMS treatment was performed. As shown in Supplementary Figure S5A, the three A residues (218–220) were sensitive to DMS treatment. Altogether, these analyses indicate that in 2A and 4A mutants, the SL-E1 helix is shortened due to mismatches induced by mutations, whereas it is restored in the 2AU mutant (Figure 2).

Change in the structure of the SL-E1 domain decreased the initiation of RNA synthesis

Next, we tried to determine which RNA synthesis step was affected by 2A and 4A mutations. RNA synthesis by NS5B polymerase can be divided into three major steps: binding of the polymerase to the RNA template, initiation and elongation of the RNA product.

We first investigated the effect of nucleotide changes on NS5B binding. Gel-shift assays were performed and the apparent k_d value (kd_{app}) was determined for WT and mutated RNAs. Similar values ranging from 519 and 579 nM were obtained for WT RNA and 2A, 4A and 2AU RNAs, indicating that the lower level of RNA synthesized from 2A and 4A RNA was not due to a lower binding of NS5B to the template (Supplementary Table S3). The same type of analysis was performed with RNA harboring mutations in the apical loop and the upper part of the stem. Comparable affinity for NS5B was found except for the 2GA mutant, which displayed a 20% higher affinity for the enzyme (Supplementary Table S3).

We next analyzed the ^{32}P-labeled RNA products synthesized from WT and mutated RNA on a denaturing polyacrylamide gel. To compare more accurately the RNA synthesized from the different templates, the same amounts of labeled products were loaded in each lane (50 000 c.p.m.). As shown in Supplementary Figure S6, WT RNA allowed the synthesis of a major 341-nt-long RNA product of the size of the template (Supplementary Figure S6 compare lanes WT and M). A band of higher molecular weight was also observed which corresponds to two successive copies of the template (24). The same migration pattern was observed when RNAs mutated in the apical loop or at different positions in the SL-E1 helix were used as templates. No arrest bands were observed during the synthesis, indicating that modification of the SL-E1 region did not induce premature termination of the elongation product.

The RNA products obtained in the above experiments were synthesized after several rounds of initiation and elongation during a 2 h incubation period. To analyze the different phases of the RNA synthesis in one round of polymerization, we performed reaction kinetics in the presence of heparin, a trapping agent allowing all polymerase molecules not involved in initiation or elongation complexes to be captured. NS5B was pre-incubated for 30 min at 25°C with WT or mutated RNAs (2A, 4A and 2AU) and the first two nucleotides to be incorporated (GTP and CTP) in order to allow the formation of stable initiation complexes. Heparin and the two other nucleotides (ATP and ^{32}P-UTP) were then added and incubation continued at the same temperature. Aliquots of the reactions were removed at different time points and ^{32}P-labeled RNA products were analyzed quantitatively and qualitatively. In these conditions, a plateau of nucleotide incorporation was observed after 20 min of incubation with the 4 RNAs (Figure 3A). The kinetic curve obtained with the 2AU mutant is indistinguishable from that obtained with WT RNA both in the initial linear phase and in the late phase. Conversely, when 2A and 4A RNAs were used as templates, both the initial velocity and the level of the plateau were reduced by about 50% compared to WT and 2AU RNAs. As no specific arrest bands were visible on the product analysis on polyacrylamide gel (Figure 3B), this result suggests that 2A and 4A mutations impede the formation of initiation complexes.

This prompted us to perform a gel-based initiation assay to quantify the amount of first di-nucleotide product synthesized from WT and 2A, 4A and 2AU mutant RNAs. The SL-E1 RNA harboring nucleotide changes in the apical loop of SL-E1 (SLE1AL RNA) was also included in this analysis. Values corresponding to the mean of three independent experiments are given in Figure 3C and a representative gel is presented in Figure 3D. It appears that the amount of initiation di-nucleotides synthesized from 2A and 4A RNAs was reduced by 49% and 40%, respectively, compared to WT RNA. Conversely, the quantity of di-nucleotides synthesized from SLE1AL and 2AU RNA was equivalent or slightly higher to that produced from WT RNA. Taken together, these results indicate that the decrease in RNA synthesis induced by structural modifications at the base

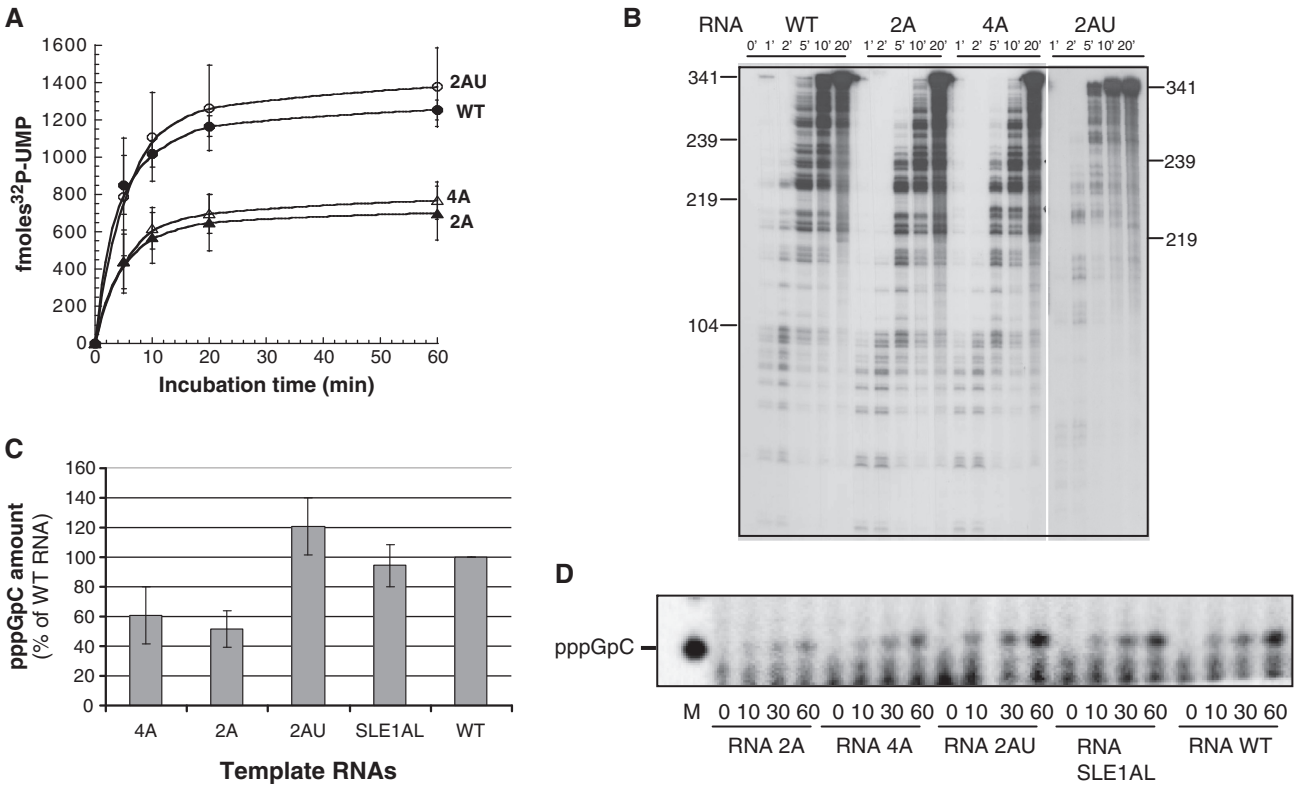

Figure 3. Some mutations in the SL-E1 stem–loop decreased initiation of RNA synthesis. For the single-round replication assay, HCV RdRp and RNA were pre-incubated for 30 min at 25°C in the reaction mixture without ATP and UTP. Heparin (MW 4000–6000 Da, 200 μg/ml) was then added followed by ATP and [^{32}P]UTP. The reaction mixture was further incubated at 25°C for 0, 5, 10, 20 and 60 min. The ^{32}P RNA products were (**A**): quantified after TCA precipitation and counted in a Wallac counter (filled circles, WT RNA; open circles, 2AU RNA; filled triangles, 2A RNA; empty triangles, 4A RNA) or (**B**): analyzed on denaturing polyacrylamide gels. For the gel-base initiation assay, an RdRp assay was performed with 0.5 mM GTP and 10 μM CTP with 4 μCi [α-^{32}P] CTP (3000 Ci × mmol^{-1}) as only added NTP. The reaction was run at 25°C for 10, 30 and 60 min. Initiation products were run in a 20% acrylamide gel in TBE buffer, submitted to electronic autoradiography using a Pharos apparatus (Biorad) and quantified using the Quantity one software (Biorad). (**C**) Quantification of initiation products synthesized with WT and mutant RNAs after 1 h incubation. Data correspond to the mean of three independent experiments ± SD. (**D**) Analysis of initiation products on polyacrylamide gel electrophoresis. M: pppGpC molecular weight marker.

of the SL-E1 stem was due to an alteration of the initiation step.

Mutation in SL-E1 stem–loop decreased RNA synthesis in Huh7 cells

In HCV-infected cells, the NS5B polymerase functions in association with a membranous complex composed of other non-structural proteins (at least NS3, NS4A, NS4B and NS5A) and cellular proteins. Interactions between the NS5B and the template could be different when the viral polymerase is included in this complex. To mimic these biological conditions more closely, we used Huh7 cells that constitutively produced the HCV replication complex from genotype 1b HCV (Huh7/Rep5.1) and an RNA minigenome containing hygromycin phosphotransferase and EGFP genes as reporter genes (5UTR-H2AE-3UTR) (30).

As the translation of the reporter gene is under the control of the HCV IRES present in the 5′UTR, we first analyzed the impact of the above-mentioned mutations on IRES-dependent translation. Indeed, nucleotide modifications introduced into the SL-E1 domain of the 3′-end of the minus strand RNA induced changes in the IIIb domain of the 5′UTR that is involved in eIF3 binding (37). This domain folds in a hairpin structure with an internal and an apical loop of 5 and 14 nt, respectively (3). Introduction of 2A or 4A mutations induced 2 or 4 GC to GU base pair changes respectively in the lower part of the IIIb helix, whereas the 2AU mutation leads to 2 GC to AU base pair changes (Figure 4A). The 2GA, 3AU, GC and SLE1AL induced nucleotide modifications of the apical loop of the IIIb region (Figure 4A). We assessed the effect of these nucleotide changes on IRES efficiency by inserting WT and mutated HCV sequences (nt 1–370) into the pIRF vector, so that HCV IRES drove initiation of RLuc translation (Figure 4B). Bicistronic capped RNA transcripts were transfected into Huh7-QR cells and luciferase activity was determined after 24 h. The mean RLuc/FLuc ratio for three independent experiments was expressed as a percentage of the ratio obtained for Huh7 transfected with bicistronic RNA containing the WT IRES sequence (Figure 4C). Sequence changes in the IIIb apical loop (3AU, GC, 2GA and SLE1AL mutants) did not alter the translation efficiency, or did so only by about 20%. With 2A and 2AU mutants bearing nucleotide changes in the IIIb helix, IRES-dependent

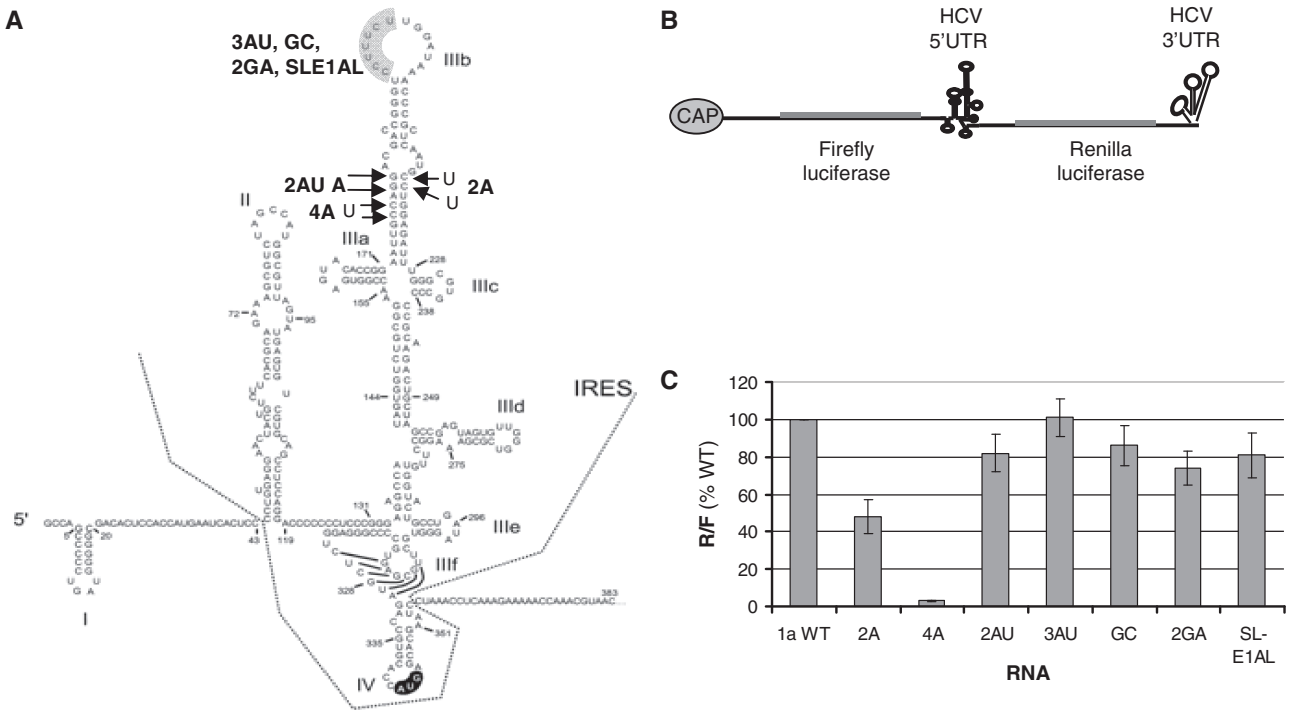

Figure 4. Effect of mutations on HCV IRES activity. (**A**) Secondary structure of HCV 5′UTR according to Honda *et al*. (45). Nucleotide changes corresponding to 2A, 4A and 2AU mutants are indicated by arrows. The sequence complementary to the apical loop of SLII of the 3′UTR is underlined in grey. (**B**) Schematic representation of bicistronic RNA produced from pIRF vector. (**C**) Bicistronic RNAs transcribed from pIRF vector containing WT or mutated HCV 5′UTR were transfected into Huh7-QR cells. The activity of each IRES was determined by calculating the ratio of RLuc to FLuc activities in cell extracts. Values are expressed as the percentage of the relative activity of the WT IRES. Each bar represents the mean value obtained in three independent experiments ± SD.

translation was reduced by 52% and 18%, respectively. The nucleotide modifications corresponding to 4A mutant completely abolished IRES-dependent translation. Consequently, the effect of this latter mutation on RNA synthesis driven by HCV RC in Huh7 cells could not be assessed.

To analyze the impact of the six other mutations on RNA replication in a cellular context, we first modified the 5′UTR and the 3′UTR sequences of the 5UTR-H2AE-3UTR minigenomes (Figure 5A). As the basal construct contained UTR sequences from the HCV Con1, we replaced both sequences by those of the H77 HCV used in the previous *in vitro* RNA synthesis. This modification did not modify the replication of the minigenome in Huh7/Rep5.1 cells (data not shown). 5UTR-H2AE-3UTR minigenomes (positive strand) containing WT or mutated 5′UTR were transfected into Huh7/Rep5.1 or in Huh7-QR cells as a control. Huh7/Rep5.1 cells were also transfected with a minigenome containing only the EGFP gene as an additional negative control (5UTR-EGFP-3UTR). Sixteen hours after transfection, the percentage of EGFP-positive cells was determined by flow cytometry to normalize the transfection efficiency. The rest of the cells were maintained in culture in the presence of 50 μg/ml hygromycin and 500 μg/ml G418. After 3 weeks, the number of resistant colonies was determined. As expected, cell colonies were never observed in hygromycin-cultured Huh7-QR cells transfected by WT $5UTR_{H77}$-H2AE-$3UTR_{H77}$ minigenome or with hygromycin-G418-cultured Huh7/Rep5.1 transfected with the 5UTR-EGFP-3UTR minigenome (Figure 5B). Conversely, with the $5UTR_{H77}$-H2AE-$3UTR_{H77}$ minigenome containing WT H77-5′UTR, 400–1500 resistant colonies per microgram of transfected RNA were obtained. A change of 1–3 nt in the apical loop of SL-E1 (3AU, GC and 2GA mutants) did not reduce the number of hygromycin-resistant colonies compared to the WT construct (Figure 5C). Even a 54% and 30% increase was observed with 3AU and 2GA minigenomes, respectively (Figure 5C). Modification of the 6 nt in the upper part of SL-E1 (sequence homologous to SLII of 3′UTR) reduced to 61% the number of resistant colonies (SLE1AL mutant). When Huh7/Rep5.1 cells were transfected with minigenomes harboring nucleotide changes that disrupt the lower helix structure of SL-E1 (2A mutant, Figure 5C), the number of hygromycin-resistant colonies was reduced to 12%. Compensatory nucleotide exchange (2AU mutant) allowed the growth of cell colonies to 80% of the wild-type level.

Finally, to assess whether the reduced number of cell colonies observed with 2A and SLE1AL minigenomes could not be attributed to a lower stability of mutated RNA minigenomes, total cellular RNAs were extracted 4 h after transfection and analyzed by northern blot with an EGFP probe. As illustrated in Figure 5D, similar amounts of 2A and SLE1AL minigenome were recovered compared to wild-type or 2GA minigenomes, ruling out the hypothesis of a lower stability of 2A and SLE1AL RNAs. Taken together, these results strongly suggest that the structure of the SL-E1 domain is important for

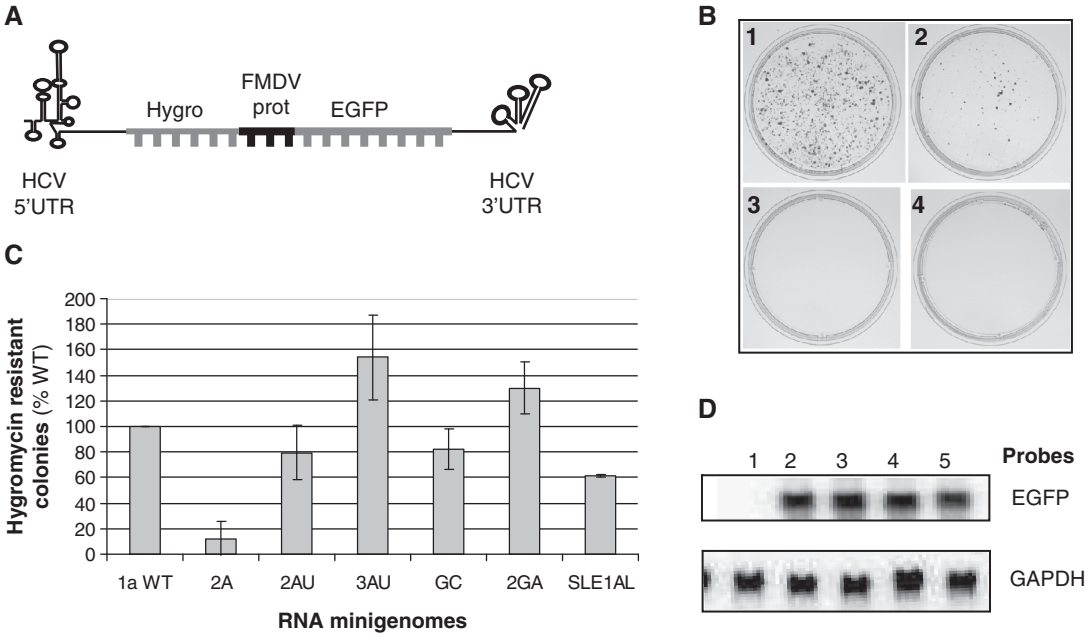

Figure 5. Some mutations in the SL-E1 stem–loop decreased RNA synthesis by RC. (**A**) Schematic representation of polycistronic RNA produced from pGEM-T/5UTR-H2AE-3UTR. FMDV prot is for FMDV 2A protease. (**B**) Polycistronic RNAs transcribed from pGEM-T/$5UTR_{H77}$-H2AE-$3UTR_{H77}$ WT or 2A or 5UTR-EGFP-3UTR were transfected into Huh7/Rep5.1 cells or Huh7-QR. After a 3-week selection, cell colonies were numbered under microscopy examination. Huh7/Rep5.1 cells transfected with $5UTR_{H77}$-H2AE-$3UTR_{H77}$ WT RNA, (1), $5UTR_{H77}$-H2AE-$3UTR_{H77}$ 2A RNA (2), 5UTR-EGFP-3UTR RNA (3) and Huh7-QR cells transfected with $5UTR_{H77}$-H2AE-$3UTR_{H77}$ WT RNA (4). (**C**) The number of hygromycin-resistant colonies was determined after transfection of WT and mutated $5UTR_{H77}$-H2AE-$3UTR_{H77}$ minigenomes in Huh7/Rep5.1 cells. Values were expressed as the percentage of the colony number obtained with the minigenome containing the WT 5′UTR. Each bar represents the mean value obtained from at least three independent experiments ± SD. (**D**) Northern blot analysis. RNAs (10 µg) of transfected Huh7/Rep5.1 cells were fractionated on 1% denaturing agarose gel and transferred to nylon membrane. Membrane-bound RNAs were hybridized with EGFP or GAPDH probes. Mock transfected cells (lane 1), cells transfected with WT minigenome (lane 2), cells transfected with 2A minigenome (lane 3), cells transfected with 2GA minigenome (lane 4), cells transfected with SLE1AL minigenome (lane 5).

efficient RNA synthesis from the 3′ sequence of the HCV minus strand RNA by NS5B, either alone or in the RC.

DISCUSSION

During the past few years, important information on the *cis*-acting elements required for replication of plus-strand RNA virus has been obtained. In the case of HCV, such elements have been mapped not only in 5′ and 3′ UTR but also in the capsid and NS5B coding sequence (18,19,38,39). *Cis*-acting elements located in the 3′UTR and in the NS5B-coding sequences are likely involved in the initiation of minus RNA synthesis from the 3′-end of the plus RNA, whereas those found in the 5′UTR and in the capsid-coding sequence are presumably involved in initiation of plus RNA synthesis from the 3′-end of minus strand RNA. The exact role of these RNA sequences in the different steps of viral RNA synthesis is poorly understood, although one RNA element (SL-V or 5BSL3.2) specifically binds the NS5B polymerase *in vitro* (38). In the 3′UTR, both the conserved 3′X sequence and the polyU-C stretch are necessary for viral replication in chimpanzee and multiplication of RNA replicon in Huh7 cells (10–12). The involvement of these sequences in RNA synthesis is unknown especially because the 3′UTR is poorly replicated by the NS5B polymerase *in vitro* and because initiation frequently occurred at internal sites (17,24,40). Conversely, the 3′-end of minus strand RNA is efficiently replicated *in vitro* by HCV polymerase that initiated on the 3′ first nucleotide of the template (24,41). Data obtained with recombinant polymerase or in the replicon system suggested that sequences and/or structures in the 104 or 125 nt at 3′-end allow a low level of replication, but that upstream sequences are necessary for efficient RNA synthesis (24–26).

To identify other RNA elements involved in RNA synthesis from this RNA domain, we analyzed the role of the SL-E1 stem–loop in RNA synthesis both *in vitro* and *in cellulo*. We chose this region for two reasons. First, antisense hybridization to this domain strongly inhibits *in vitro* RNA synthesis (36). Second, the upper part of this structure displays a common feature with the SL-II stem–loop of the 3′UTR with an identical 6-nt sequence (21,22). Our data indicated that nucleotide changes that destabilized the lower part of the SL-E1 stem reduced RNA synthesis catalyzed by recombinant NS5B by a factor 2, whereas the level of RNA synthesis remained constant or increased slightly when mutations were introduced into the sequence homologous to SL-II. The change in the SL-E1 hairpin structure did not decrease NS5B binding or induce any modification of the initiation site or polymerase dissociation during elongation. Surprisingly, it reduced the formation of the functional initiation complex, even though this RNA region is distant from the 3′end of the template (nt 177–222).

The data reported here does not allow us to determine the role of this domain in initiation. Gel-shift experiments showed no differences in enzyme affinity between WT RNA or 2A and 4A mutant RNA that would have caused inefficient initiation. However, it cannot be excluded that subtle interactions occurred between NS5B and the SL-E1 stem–loop after the correct positioning of the first 2 nt, before the formation of the first phospho-diester bond. Modifications of the SL-E1 domain could also induce changes in the tertiary structure of the 341-nt fragment, which may alter the ratio of productive and unproductive initiation complex. In this regard, it should be noted that introduction of a C224U nucleotide change, which is specifically found in RNA from genotype 3 HCV, into a genotype 1 sequence also induced a 2-fold reduction of RNA synthesis from the 3′-end of minus strand model RNAs (42). *In silico* secondary structure predictions indicated that this modification led to a 3-base lengthening of the SL-E1 stem without affecting the secondary structure of other RNA domains. Further experiments using surface plasmon resonance UV-monitored spectroscopy could help to determine more precisely the interaction between NS5B and the WT or mutant RNAs in the presence or in the absence of NTP.

Before testing the effect of SL-E1 mutations on RNA synthesis in a cellular context, we evaluated their impact on translation from the 5′UTR using a bicistronic reporter construct. Indeed, during RNA replication, the nucleotide changes introduced into the SL-E1 stem–loop of the 3′-end of minus strand RNA induced nucleotide changes in the IIIb domain of the HCV IRES. The latter has been shown to contain a critical determinant of eIF3 binding (37). Inversion of the apical loop sequence or replacement of the HCV loop by the BVDV loop reduced the IRES translation efficiency by 2-fold (37,43). We found that the IIIb loop modification corresponding to nucleotide changes of the sequence homologous to the SLII loop of the 3′UTR did not modify or only slightly modified the translation level (Figure 4: 3AU, GC, 2GA and SLE1AL mutants). The replacement of two or four GC base pairs by two or four GU base pairs in the IIIb stem (2A or 4A mutants) led to about a 2-fold or total reduction of translation, respectively. Conversely, replacing the two GU base pairs corresponding to the 2A mutant with two AU base pairs (2AU mutant) restored the translation level to 82% of WT translation (Figure 4C).

We then evaluated the effect of mutations in the SL-E1 stem–loop on viral RNA synthesis in a cellular context mimicking viral RNA replication in HCV-infected cells. To this end, we used a minigenome system developed in our laboratory (30) because in this cellular model the synthesis of the HCV nonstructural proteins is independent of translation and replication of the minigenome driven by HCV UTR sequences. Consequently, a lower minigenome replication could not be attributed to a decrease in the RC amount in Huh7 cells. This allowed us to demonstrate that the intact structure of the SL-E1 stem–loop contributes to efficient RNA synthesis from the 3′-end of HCV minus strand RNA by the viral replication complex. Indeed, mutations that destabilize the lower part of the stem led to an 8-fold reduction of hygromycin-resistant cell clones (Figure 5C, 2A mutant), whereas compensatory mutations restored the number of resistant clones to almost the WT level (Figure 5C, 2AU mutant). It could be argued that the lower amount of resistant colonies obtained with 2A minigenome resulted from a lower hygromycin-phosphotransferase production due to its lower IRES activity (48%, Figure 4) rather than from a decrease in RNA synthesis. This hypothesis is unlikely, however, since previous data indicated that WT IRES activity allowed the production of a sufficient amount of hygromycin-phosphotransferase to confer resistance to 300 μg/ml hygromycin (30). As all the results reported here were obtained after selection in 50 μg/ml hygromycin, the translation decrease induced by 2A mutations should not affect the minigenome capacity to confer cell resistance to the antibiotic.

The role of the sequence shared by SL-E1 and SLII of 3′UTR in viral RNA synthesis is less clear. Modification of 1–3 nt in this sequence did not significantly hamper minigenome replication (GC minigenome) or even induce a slight increase (3AU and 2GA minigenomes). It should be noted that the two latter mutations also induced a small increase in *in vitro* RNA synthesis. These results are in agreement with those previously reported by Grassmann *et al.* (43) who showed a moderate effect of mutations in the apical loop of the IIIb domain using different nucleotide changes and a replicon system. However, when all 6 nt of the sequence homologous to SLII of the 3′UTR were changed simultaneously (SLE1AL mutant), the replication level of the minigenome decreased by 39% compared to WT. The effect of the SLE1AL mutation was different when RNA synthesis was performed in Huh7 cells by the HCV replication complex or *in vitro* by the purified NS5B. In the latter case, SLE1AL mutations had no effect (Figure 1B). Interactions of this sequence with other viral or cellular components of the replication complex in Huh7 cells could explain this difference. During the preparation of this manuscript, Friebe and Bartenschlager (44) published a paper reporting the effect of large deletion in different domains of the HCV 5′-end on the replication of chimeric replicons in Huh7 cells. In agreement with the data reported here, they showed that the SL-E1 domain is an auxiliary element for replication. Our site-directed mutagenesis study confirmed that the reduced replication is due to structure modifications rather than changes in the primary sequence of the RNA. In addition, we demonstrate that, at least *in vitro*, this alteration affects the initiation step of the viral RNA synthesis. This result makes this RNA domain an attractive target for the development of antiviral molecules directed against RNA elements such as antisense oligonucleotides, aptamers or siRNAs. The fact that antisense oligonucleotides against a part of this RNA domain completely inhibited *in vitro* RNA synthesis catalyzed by HCV NS5B (36) suggests that drugs targeting this RNA domain could be included in anti-HCV treatments.

SUPPLEMENTARY DATA

Supplementary Data are available at NAR Online.

ACKNOWLEDGEMENTS

We thank Dr Jens Bukh (Department of Infectious Diseases and Clinical Research Center, Copenhagen) for providing the pCV-J4L6 molecular clone and Dr Ralf Bartenschlager (University of Heidelberg) for providing the Rep5.1 replicon. We are grateful to Drs Michel Castroviejo, Marie-Line Andreola and Christian Cazenave (CNRS Bordeaux) for helpful discussions.

FUNDING

The Agence Nationale de Recherche contre le Sida (ANRS, grant number 06033/07028); Centre National de la Recherche Scientifique (CNRS); University Victor Segalen Bordeaux 2. a Ph.D. fellowship from the ANRS (to K.M.); Ph.D fellowship from the Egyptian Ministry of Education (to N.A-El-S.). Funding for open access charge: CNRS.

Conflict of interest statement. None declared.

REFERENCES

1. Choo,Q.L., Kuo,G., Weiner,A.J., Overby,L.R., Bradley,D.W. and Houghton,M. (1989) Isolation of a cDNA clone derived from a blood-borne non-A, non-B viral hepatitis genome. *Science*, **244**, 359–362.
2. Penin,F., Dubuisson,J., Rey,F.A., Moradpour,D. and Pawlotsky,J.M. (2004) Structural biology of hepatitis C virus. *Hepatology*, **39**, 5–19.
3. Honda,M., Ping,L.H., Rijnbrand,R.C., Amphlett,E., Clarke,B., Rowlands,D. and Lemon,S.M. (1996) Structural requirements for initiation of translation by internal ribosome entry within genome-length hepatitis C virus RNA. *Virology*, **222**, 31–42.
4. Moriishi,K. and Matsuura,Y. (2007) Host factors involved in the replication of hepatitis C virus. *Rev. Med. Virol.*, **17**, 343–354.
5. Egger,D., Wolk,B., Gosert,R., Bianchi,L., Blum,H.E., Moradpour,D. and Bienz,K. (2002) Expression of hepatitis C virus proteins induces distinct membrane alterations including a candidate viral replication complex. *J. Virol.*, **76**, 5974–5984.
6. Gosert,R., Egger,D., Lohmann,V., Bartenschlager,R., Blum,H.E., Bienz,K. and Moradpour,D. (2003) Identification of the hepatitis C virus RNA replication complex in huh- 7 cells harboring subgenomic replicons. *J. Virol.*, **77**, 5487–5492.
7. Behrens,S.E., Tomei,L. and De Francesco,R. (1996) Identification and properties of the RNA-dependent RNA polymerase of hepatitis C virus. *EMBO J.*, **15**, 12–22.
8. Lohmann,V., Korner,F., Herian,U. and Bartenschlager,R. (1997) Biochemical properties of hepatitis C virus NS5B RNA-dependent RNA polymerase and identification of amino acid sequence motifs essential for enzymatic activity. *J. Virol.*, **71**, 8416–8428.
9. Lohmann,V., Korner,F., Koch,J., Herian,U., Theilmann,L. and Bartenschlager,R. (1999) Replication of subgenomic hepatitis C virus RNAs in a hepatoma cell line. *Science*, **285**, 110–113.
10. Yanagi,M., St Claire,M., Emerson,S.U., Purcell,R.H. and Bukh,J. (1999) In vivo analysis of the 3′ untranslated region of the hepatitis C virus after in vitro mutagenesis of an infectious cDNA clone. *Proc. Natl Acad. Sci. USA*, **96**, 2291–2295.
11. Friebe,P. and Bartenschlager,R. (2002) Genetic analysis of sequences in the 3′ nontranslated region of hepatitis C virus that are important for RNA replication. *J. Virol.*, **76**, 5326–5338.
12. Yi,M. and Lemon,S.M. (2003) 3′ nontranslated RNA signals required for replication of hepatitis C virus RNA. *J. Virol.*, **77**, 3557–3568.
13. Luo,G., Hamatake,R.K., Mathis,D.M., Racela,J., Rigat,K.L., Lemm,J. and Colonno,R.J. (2000) De novo initiation of RNA synthesis by the RNA-dependent RNA polymerase (NS5B) of hepatitis C virus. *J. Virol.*, **74**, 851–863.
14. Hong,Z., Cameron,C.E., Walker,M.P., Castro,C., Yao,N., Lau,J.Y. and Zhong,W. (2001) A novel mechanism to ensure terminal initiation by hepatitis c virus ns5b polymerase. *Virology*, **285**, 6–11.
15. Cheney,I.W., Naim,S., Lai,V.C., Dempsey,S., Bellows,D., Walker,M.P., Shim,J.H., Horscroft,N., Hong,Z. and Zhong,W. (2002) Mutations in NS5B polymerase of hepatitis C virus: impacts on in vitro enzymatic activity and viral RNA replication in the subgenomic replicon cell culture. *Virology*, **297**, 298–306.
16. Ranjith-Kumar,C.T., Sarisky,R.T., Gutshall,L., Thomson,M. and Kao,C.C. (2004) De novo initiation pocket mutations have multiple effects on hepatitis C virus RNA-dependent RNA polymerase activities. *J. Virol.*, **78**, 12207–12217.
17. Oh,J.W., Sheu,G.T. and Lai,M.M. (2000) Template requirement and initiation site selection by hepatitis C virus polymerase on a minimal viral RNA template. *J. Biol. Chem.*, **275**, 17710–17717.
18. You,S., Stump,D.D., Branch,A.D. and Rice,C.M. (2004) A cis-acting replication element in the sequence encoding the NS5B RNA-dependent RNA polymerase is required for hepatitis C virus RNA replication. *J. Virol.*, **78**, 1352–1366.
19. Friebe,P., Boudet,J., Simorre,J.P. and Bartenschlager,R. (2005) Kissing-loop interaction in the 3′ end of the hepatitis C virus genome essential for RNA replication. *J. Virol.*, **79**, 380–392.
20. Diviney,S., Tuplin,A., Struthers,M., Armstrong,V., Elliott,R.M., Simmonds,P. and Evans,D.J. (2008) A hepatitis C virus cis-acting replication element forms a long-range RNA-RNA interaction with upstream RNA sequences in NS5B. *J. Virol.*, **82**, 9008–9022.
21. Schuster,C., Isel,C., Imbert,I., Ehresmann,C., Marquet,R. and Kieny,M.P. (2002) Secondary structure of the 3′ terminus of hepatitis C virus minus- strand RNA. *J. Virol.*, **76**, 8058–8068.
22. Smith,R.M., Walton,C.M., Wu,C.H. and Wu,G.Y. (2002) Secondary structure and hybridization accessibility of hepatitis C virus 3′-terminal sequences. *J. Virol.*, **76**, 9563–9574.
23. Dutkiewicz,M., Swiatkowska,A., Figlerowicz,M. and Ciesiolka,J. (2008) Structural domains of the 3′-terminal sequence of the hepatitis C virus replicative strand. *Biochemistry*, **47**, 12197–12207.
24. Reigadas,S., Ventura,M., Sarih-Cottin,L., Castroviejo,M., Litvak,S. and Astier-Gin,T. (2001) HCV RNA-dependent RNA polymerase replicates in vitro the 3′ terminal region of the minus-strand viral RNA more efficiently than the 3′ terminal region of the plus RNA. *Eur. J. Biochem.*, **268**, 5857–5867.
25. Astier-Gin,T., Bellecave,P., Litvak,S. and Ventura,M. (2005) Template requirements and binding of hepatitis C virus NS5B polymerase during in vitro RNA synthesis from the 3′-end of virus minus-strand RNA. *FEBS J.*, **272**, 3872–3886.
26. Friebe,P., Lohmann,V., Krieger,N. and Bartenschlager,R. (2001) Sequences in the 5′ nontranslated region of hepatitis C virus required for RNA replication. *J. Virol.*, **75**, 12047–12057.
27. Kim,Y.K., Kim,C.S., Lee,S.H. and Jang,S.K. (2002) Domains I and II in the 5′ nontranslated region of the HCV genome are required for RNA replication. *Biochem. Biophys. Res. Commun.*, **290**, 105–112.
28. Yanagi,M., Purcell,R.H., Emerson,S.U. and Bukh,J. (1997) Transcripts from a single full-length cDNA clone of hepatitis C virus are infectious when directly transfected into the liver of a chimpanzee. *Proc. Natl Acad. Sci. USA*, **94**, 8738–8743.
29. Dutartre,H., Boretto,J., Guillemot,J.C. and Canard,B. (2005) A relaxed discrimination of 2′-O-methyl-GTP relative to GTP between de novo and elongative RNA synthesis by the hepatitis C RNA-dependent RNA polymerase NS5B. *J. Biol. Chem.*, **280**, 6359–6368.
30. Dumas,E., Masante,C., Astier-Gin,T., Lapaillerie,D. and Ventura,M. (2007) The hepatitis C virus minigenome: a new cellular model for studying viral replication. *J. Virol. Methods*, **142**, 59–66.
31. Krieger,N., Lohmann,V. and Bartenschlager,R. (2001) Enhancement of hepatitis C virus RNA replication by cell culture-adaptive mutations. *J. Virol.*, **75**, 4614–4624.

32. Laporte,J., Malet,I., Andrieu,T., Thibault,V., Toulme,J.J., Wychowski,C., Pawlotsky,J.M., Huraux,J.M., Agut,H. and Cahour,A. (2000) Comparative analysis of translation efficiencies of hepatitis C virus 5′ untranslated regions among intraindividual quasispecies present in chronic infection: opposite behaviors depending on cell type. *J. Virol.*, **74**, 10827–10833.
33. Dumas,E., Staedel,C., Colombat,M., Reigadas,S., Chabas,S., Astier-Gin,T., Cahour,A., Litvak,S. and Ventura,M. (2003) A promoter activity is present in the DNA sequence corresponding to the hepatitis C virus 5′ UTR. *Nucleic Acids Res.*, **31**, 1275–1281.
34. Kashiwagi,T., Hara,K., Kohara,M., Kohara,K., Iwahashi,J., Hamada,N., Yoshino,H. and Toyoda,T. (2002) Kinetic analysis of C-terminally truncated RNA-dependent RNA polymerase of hepatitis C virus. *Biochem. Biophys. Res. Commun.*, **290**, 1188–1194.
35. van Leeuwen,H.C., Reusken,C.B., Roeten,M., Dalebout,T.J., Riezu-Boj,J.I., Ruiz,J. and Spaan,W.J. (2004) Evolution of naturally occurring 5′ non-translated region variants of hepatitis C virus genotype 1b in selectable replicons. *J. Gen. Virol.*, **85**, 1859–1866.
36. Reigadas,S., Ventura,M., Andreola,M.L., Michel,J., Gryaznov,S., Tarrago-Litvak,L., Litvak,S. and Astier-Gin,T. (2003) An oligonucleotide complementary to the SL-B1 domain in the 3′-end of the minus-strand RNA of the hepatitis C virus inhibits in vitro initiation of RNA synthesis by the viral polymerase. *Virology*, **314**, 206–220.
37. Kieft,J.S., Zhou,K., Jubin,R. and Doudna,J.A. (2001) Mechanism of ribosome recruitment by hepatitis C IRES RNA. *RNA*, **7**, 194–206.
38. Lee,H., Shin,H., Wimmer,E. and Paul,A.V. (2004) cis-acting RNA signals in the NS5B C-terminal coding sequence of the hepatitis C virus genome. *J. Virol.*, **78**, 10865–10877.
39. McMullan,L.K., Grakoui,A., Evans,M.J., Mihalik,K., Puig,M., Branch,A.D., Feinstone,S.M. and Rice,C.M. (2007) Evidence for a functional RNA element in the hepatitis C virus core gene. *Proc. Natl Acad. Sci. USA*, **104**, 2879–2884.
40. Pellerin,C., Lefebvre,S., Little,M.J., McKercher,G., Lamarre,D. and Kukolj,G. (2002) Internal initiation sites of de novo RNA synthesis within the hepatitis C virus polypyrimidine tract. *Biochem. Biophys. Res. Commun.*, **295**, 682–688.
41. Oh,J.W., Ito,T. and Lai,M.M. (1999) A recombinant hepatitis C virus RNA-dependent RNA polymerase capable of copying the full-length viral RNA. *J. Virol.*, **73**, 7694–7702.
42. Masante,C., Mahias,K., Lourenco,S., Dumas,E., Cahour,A., Trimoulet,P., Fleury,H., Astier-Gin,T. and Ventura,M. (2008) Seven nucleotide changes characteristic of the hepatitis C virus genotype 3 5′ untranslated region: correlation with reduced in vitro replication. *J. Gen. Virol.*, **89**, 212–221.
43. Grassmann,C.W., Yu,H., Isken,O. and Behrens,S.E. (2005) Hepatitis C virus and the related bovine viral diarrhea virus considerably differ in the functional organization of the 5′ non-translated region: implications for the viral life cycle. *Virology*, **333**, 349–366.
44. Friebe,P. and Bartenschlager,R. (2009) Role of RNA structures in genome terminal sequences of the hepatitis C virus for replication and assembly. *J. Virol.*, **83**, 11989–11995.
45. Honda,M., Beard,M.R., Ping,L.H. and Lemon,S.M. (1999) A phylogenetically conserved stem-loop structure at the 5′ border of the internal ribosome entry site of hepatitis C virus is required for cap-independent viral translation. *J. Virol.*, **73**, 1165–1174.